Stochastic Acid-Base Quenching in Chemically Amplified Photoresists: A Simulation Study

Chris A. Mack[a)], John J. Biafore[b)], Mark D. Smith[b)]

a) *Lithoguru.com, 1605 Watchhill Rd, Austin, TX 78703*
b) *KLA-Tencor, FINLE Division, 8843 N. Capital of Texas Highway, Austin, TX 78759*

Abstract

BACKGROUND: The stochastic nature of acid-base quenching in chemically amplified photoresists leads to variations in the resulting acid concentration during post-exposure bake, which leads to line-edge roughness (LER) of the resulting features.
METHODS: Using a stochastic resist simulator, we predicted the mean and standard deviation of the acid concentration after post-exposure bake for an open-frame exposure and fit the results to empirical expressions.
RESULTS: The mean acid concentration after quenching can be predicted using the reaction-limited rate equation and an effective rate constant. The effective quenching rate constant is predicted by an empirical expression. A second empirical expression for the standard deviation of the acid concentration matched the output of the PROLITH stochastic resist model to within a few percent
CONCLUSIONS: Predicting the stochastic uncertainty in acid concentration during post-exposure bake for 193-nm and extreme ultraviolet resists allows optimization of resist processing and formulations, and may form the basis of a comprehensive LER model.

Keywords: Stochastic modeling, EUV photoresist, reaction-diffusion, quenching, line-edge roughness, linewidth roughness, LER, LWR

I. INTRODUCTION

The kinetics of post-exposure bake (PEB) reaction and diffusion in chemically amplified resists plays an important role in determining the line-edge roughness (LER) of the final lithographic features. The diffusion of acid smoothes out high-frequency roughness with a correlation length related to the diffusion length.[1] Diffusion, however, reduces the deprotection gradient, causing an increase in LER. As a result, an optimum acid diffusion length will give a minimum LER. Additionally, the role of quencher is known to be critical to the magnitude of LER. Higher amounts of quencher cause an increase in the uncertainty in the amount of deprotection taking place, but an even greater increase in the gradient of deprotection, resulting in an improvement in LER.[2] Unfortunately, the complex interactions of acid diffusion, quencher loading, and quencher diffusion on LER has yet to be fully quantified. Thus, while we suspect there to be an optimum quencher concentration that minimizes LER, our stochastic theories do not yet allow us to find this optimum.

In this paper, the stochastic resist model (SRM) in PROLITH X3.2 is used to study the impact of acid and quencher amounts and diffusion on the relative uncertainty in acid concentration during PEB due to stochastic effects. By varying the exposure dose for an open-frame exposure, the relative uncertainty in the acid concentration remaining after PEB ($\sigma_h / \langle h \rangle$) as a function of the mean acid concentration ($\langle h \rangle$) will be simulated for varying amounts of quencher, and for differing diffusivities of both acid and quencher. These results will then be described by simple, approximate equations that provide analytical prediction of acid uncertainty. The result will be useful for optimizing resist formulations and processes for minimum LER.

II. THEORY AND BACKGROUND

a. Reaction-limited vs. Diffusion-limited Systems

Consider a sealed vessel where particles of two different species undergo a reaction process in an inert solvent. The motion of the particles is Brownian, due to thermal bombardment of the solvent molecules. We are interested in the reaction kinetics or the time dependencies of the concentrations of the reactants and the products. The reaction kinetics are governed by two time scales, the diffusion time τ_{DIFF} or the typical time for two particles in the reaction volume to collide with each other, and the reaction time τ_{REACT} or the typical time for two particles to react when held in close proximity (within the reaction radius) of each other.

When $\tau_{DIFF} \ll \tau_{REACT}$, the process is slowed by the comparatively large reaction time and the system is said to be *reaction-limited* or *reaction-controlled*. Particles may travel within the reaction radius (collide) several times before reacting. The particles may sample a relatively large volume of the sealed vessel before undergoing reaction. In this case, the local fluctuations in concentration are ignored, $\tau_{DIFF} \sim 0$ and the overall rate of the process R, the number of reaction events per unit volume per unit time, can be calculated by considering the global concentrations of the reactants:

$$R = k \prod_{i=1}^{n} c_i^{N_i} \tag{1}$$

where c_i is the global concentration of the i^{th} species, N_i is the number of particles of the i^{th} species participating in one reaction event (also known as the stoichiometric coefficient), k is the reaction constant that scales as $\sim 1/\tau_{REACT}$, and n is the number of species. Equation (1) is an example of a classical mean-field rate equation.

Conversely, when $\tau_{DIFF} \gg \tau_{REACT}$, the process is *diffusion-limited* or *diffusion-controlled*. Particles react most likely upon their first encounter and the overall rate is influenced by local fluctuations in the concentration of the reactants and also by the properties of the diffusion process. In this case, one can no longer (completely) rely on classical rate equations which depend on global concentrations. Reactions in condensed media are most often diffusion-limited, a property which affects the kinetics of many dynamic processes to some extent.

One way to partially account for fluctuations is by subdividing the space into cells and replacing the global concentration of the reactants with local densities:

$$\rho_i = \frac{\langle n_i \rangle}{V} \tag{2}$$

where $\langle n_i \rangle$ is the average number of particles of type i in a cell of volume V. Over time, the number of particles will change due to reactions within the cell and also due to the diffusion of particles to and from other cells. The diffusion time within a cell is a function of the size of the cell. If the cells are small enough, we might treat reactions inside cells using classical rate equations. In this case, the concentrations are described by a *reaction-diffusion* equation

$$\frac{\partial \rho_i}{\partial t} = D_i \nabla^2 \rho_i + R(\rho_j) \tag{3}$$

where D_i is the diffusion constant of species i and ∇^2 is the Laplacian operator. The first term on the right-hand side (RHS) represents the diffusion of species i to/from adjacent cells. The second term on the RHS represents the reactions which occur within the cell with species j. R is a function representing a classical mean-field rate equation of the same form as equation (1).

A difficulty with using reaction-diffusion equations comes to light as a consequence of local fluctuations in the number of reactants. The density ρ represents the average number of particles $\langle n \rangle$ in a cell averaged over many randomized trials, but ignores fluctuations from this average $\langle n^2 \rangle - \langle n \rangle^2$. If n is large enough then the fluctuations are negligible; therefore, cells ought to be made small enough to justify the use of classical rate equations for reactions within the cell, yet large enough to minimize the effects of fluctuations. This is a difficult compromise.

a. The Two-Species Annihilation Reaction

The following discussion follows the treatment given by D. ben-Avraham and S. Havlin.[3] Consider a two-species annihilation reaction of the sort $A + B \rightarrow 0$. Instead of annihilation, we may imagine that the product of *A* and *B* is an inert species that doesn't affect the kinetics, such as irreversible acid-base quenching that produces an inert salt. In the reaction-limited regime, the mean-field rate equations are

$$\frac{dc_A}{dt} = -kc_Ac_B \qquad \frac{dc_B}{dt} = -kc_Bc_A \tag{4}$$

As the reaction proceeds, it's interesting to note that the difference between the concentrations of the two species is constant

$$\frac{dc_A}{dt} - \frac{dc_B}{dt} = 0 \tag{5}$$

$$c_A(t) - c_B(t) = constant = c_A(0) - c_B(0) \tag{6}$$

The concentration of the minority species (the species with smaller initial concentration) may be calculated from a solution to the reaction-limited rate equation:

$$c = \frac{c_0\delta_0 e^{-k\delta_0 t}}{(c_0 + \delta_0) - c_0 e^{-k\delta_0 t}} \tag{7}$$

where c_0 is the t = 0 concentration, and $\delta_0 \equiv |c_A(0) - c_B(0)|$. In the special case of $c_A(0) = c_B(0)$, the decay becomes

$$c = \frac{c_0}{1 + c_0 kt} \tag{8}$$

In the diffusion-limited regime, the $A + B \rightarrow 0$ reaction brings to light the role of spatial fluctuations in the local concentration of the reactants. Imagine that the initial concentrations of both *A* and *B* are equal and let both *A* and *B* diffuse with an equal diffusion coefficient *D*. In a volume *V*, the initial number of *A* particles will be

$$N_A(0) = c_A(0)\,V \pm \sqrt{c_A(0)\,V} \tag{9}$$

The second term on the RHS represents an estimation of the uncertainty in the number of *A* particles initially (assuming $N_A(0)$ is Poisson distributed). Because the difference between the number of particles is conserved, at the end of the process there will be left in our region about $\sqrt{c_A(0)V}$ unreacted particles. The spatial distribution of the particles is of interest and may be investigated by Monte Carlo simulation. The simple rules for simulation are as follows. The simulation domain is subdivided into cells. Only one particle is allowed to occupy a cell at any given time. Initially, each cell of the lattice is randomly populated with either an *A* or *B* particle with equal probability. Particles are then allowed to hop with equal probability to one of the four adjacent cells. A hop to a cell containing a particle of the opposite species results in the removal of both particles from the system. A hop to a cell containing a particle of like species is disallowed. The boundaries are flux-conservative, such that if a particle hops off the lattice, it re-enters the lattice on the opposite side. Figure 1 shows a Monte Carlo simulation of the $A + B \rightarrow 0$ diffusion-limited reaction in two dimensions after 5×10^5 time steps.

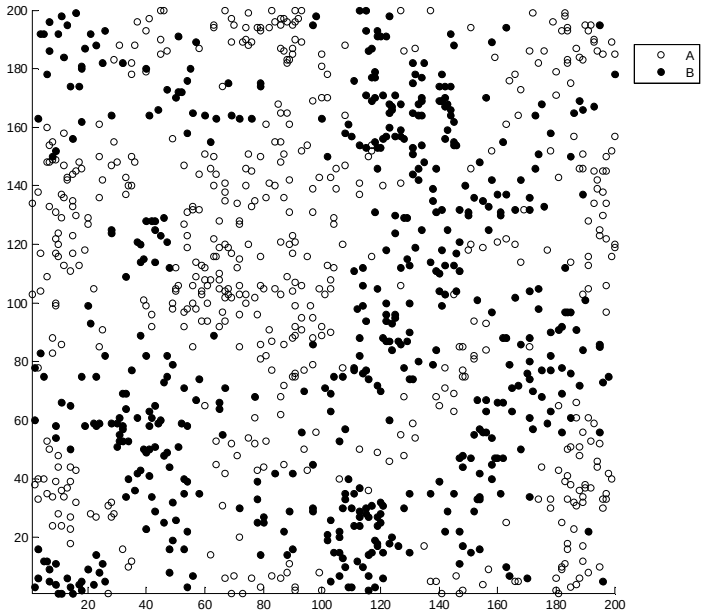

Figure 1. Monte Carlo simulation of the $A + B \rightarrow 0$ reaction in the diffusion-limited regime. Shown is the state of a 200 x 200 lattice after 5×10^5 steps. All sites were initially filled with either *A* or *B* particles, with equal probability. The segregation into *A*-rich and *B*-rich domains is clearly visible.

As the reaction proceeds, the formation of alternating domains of *A*-rich and *B*-rich particles can be clearly observed. This *segregation* phenomenon is an example of complex pattern formation which arises naturally in several reaction-diffusion systems.[4] Segregation has the effect of slowing the overall rate of the annihilation process, since reactions between *A* and *B* particles can only take place at the boundary between domains. Figure 2 shows an attempt to use equation (8), the reaction-limited rate equation, to model the results of Monte Carlo simulation in the diffusion limited regime. The reaction-limited rate equation does not predict the slowing of the reaction due to segregation effects.

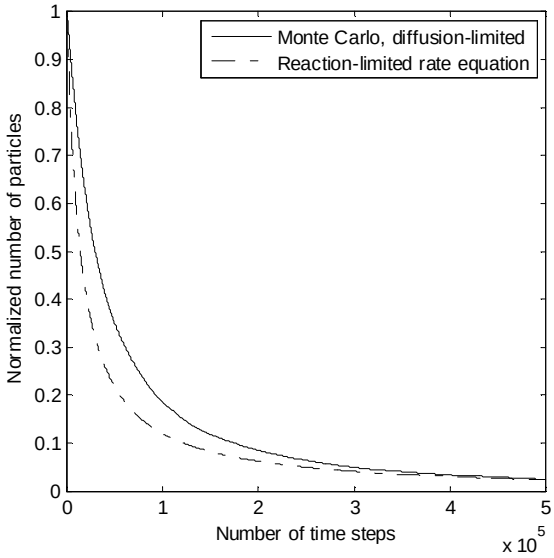

Figure 2. Modeling the $A + B \rightarrow 0$ reaction in the diffusion-limited regime and the reaction-limited regime. Shown are the normalized number of surviving *B* particles in a 200 x 200 lattice computed by Monte Carlo simulation (solid line) and by a reaction-limited rate equation (dotted line) versus the number of time steps. The rate equation is unable to predict the slowing of the reaction due to segregation phenomena.

b. Diffusion-Limited Neutralization in Chemically-Amplified Resists

Most modern chemically-amplified resists include in their formulation the addition of a (basic) quencher. Loaded at a fraction of the PAG concentration, the intent of quencher (Q) is the neutralization of any encountered photogenerated acid (H).

$$H + Q \xrightarrow{K_{EQ}} HQ \tag{10}$$

Acid-base neutralization reactions tend to be equilibrium reactions, but in this case the equilibrium constant K_{EQ} is large due to the strength of the acid, meaning that the reaction heavily favors formation of the acid-base pair HQ. Thus, it's a reasonable approximation to replace the equilibrium constant with a standard forward reaction rate constant, k_Q. If the product HQ is inert, then

$$H + Q \xrightarrow{k_Q} 0 \tag{11}$$

The description of neutralization in CARs is complicated by the fact that both photogenerated acid and quencher diffuse during the post-exposure bake process. Accordingly, the (coupled) reaction-diffusion equations for the case of constant diffusivity are

$$\frac{\partial H}{\partial t} = D\nabla^2 H - k_Q HQ \tag{12}$$

$$\frac{\partial Q}{\partial t} = D\nabla^2 Q - k_Q QH \tag{13}$$

III. SIMULATION RESULTS – MEAN ACID CONCENTRATION

In this paper a simulator using Monte Carlo, statistical-mechanical techniques called the PROLITH Stochastic Resist Model (version X3.2, from KLA-Tencor) is used to model both the mean and standard deviation of the acid concentration after post-exposure bake (PEB) for the simple case of a large open-frame exposure. In a separate paper[5], analytical expressions to predict the mean and standard deviation of the acid concentration after EUV exposure were found to be accurate compared to PROLITH SRM simulations to within 1% for typical conditions.

$$C = d_e \alpha \phi_e \phi_{PAG} \sigma_{e-PAG} \left(\frac{\lambda}{hc} \right)$$

$$d_e = d_0 \left(1 - \frac{IP}{110eV} \right)$$

$$\sigma_{e-PAG} = \pi (r - r_o)^2 \qquad r_o = 0.0084 E_{excit}^2$$

$$\frac{\sigma_h^2}{\langle h \rangle^2} = \frac{1}{\langle h \rangle \langle n_{0-PAG} \rangle} + \left(\frac{(1 - \langle h \rangle) \ln(1 - \langle h \rangle)}{\langle h \rangle} \right)^2 \frac{1}{\langle n_{photoelectrons} \rangle}$$

$$\langle n_{photoelectrons} \rangle = \phi_e \langle n_{photons} \rangle (1 - e^{-\alpha D}) \qquad \langle h \rangle = 1 - e^{-C \langle E \rangle}$$

where C = exposure rate constant
d_e = mean effective electron path length
α = resist absorption coefficient
ϕ_e = secondary electron generation efficiency
ϕ_{PAG} = PAG quantum efficiency
$\sigma_{e\text{-}PAG}$ = electron-PAG reaction cross-section
λ = exposure wavelength
h = Planck's constant
c = vacuum speed of light
d_o = mean effective electron path length when the ionization potential is zero = 4.75 nm
IP = resist ionization potential
r = PAG reaction radius
r_o = minimum PAG reaction radius
E_{excit} = PAG excitation energy
σ_h = standard deviation of the relative acid concentration for a given volume of resist
$\langle h \rangle$ = mean relative acid concentration in a given volume
$\langle n_{0-PAG} \rangle$ = mean initial number of PAGs in a given volume
$\langle n_{photoelectrons} \rangle$ = mean number of photoelectrons generated in a given volume
$\langle n_{photons} \rangle$ = mean number of photons incident on a given volume
D = resist thickness
$\langle E \rangle$ = mean exposure dose

This same simulator is now used to examine the stochastic behavior of acid-base quenching. The baseline values of the parameters for the simulations in this paper are given in Table I. These values result in an exposure rate constant of C = 0.08652 cm^2/mJ.

Table I: Baseline stochastic resist parameters for EUV simulations

PAG Molar Absorptivity	0
Initial PAG Density, ρ_{PAG}	0.2 /nm^3
Absorption Coefficient, α	0.006516 nm^{-1}
Electron Generation Efficiency, ϕ_e	0.9
Ionization Potential, *IP*	10 eV
PAG Excitation Radius, *r*	2.0 nm
PAG Excitation Energy, E_{excit}	5 eV
PAG Quantum Efficiency, ϕ_{PAG}	0.5
Open frame area	50 nm X 50 nm
Resist thickness	10 nm
Initial Quencher Density, ρ_Q	0.05 /nm^3
Acid-Base Quenching Rate Constant	15 nm^3/s^{-1}
Acid Diffusivity, D_A	1 nm^2/s
Base Diffusivity, D_Q	1 nm^2/s
PEB Time, t_{PEB}	25 s

Ideally, every quencher finds an acid during PEB and is neutralized (here, our attention will be limited to the cases where sufficient dose is used so that there is an excess of acid). Letting G_0 = the concentration of PAG before exposure, Q_0 = the initial concentration of quencher (at the start of PEB), H_0 = the acid concentration at the start of PEB, Q = the concentration of quencher at the end of PEB, and H = the acid concentration at the end of PEB, it will be convenient to define relative concentrations:

$$q_0 = \frac{Q_0}{G_0}\ , \quad h_0 = \frac{H_0}{G_0}\ , \quad q = \frac{Q}{G_0}\ , \quad h = \frac{H}{G_0} \tag{14}$$

For complete quenching, the stoichiometry gives $h = \delta_0 \equiv h_0 - q_0$. Note that for the parameters of Table I, $\delta_0 = 0$ requires a dose of 3.43 mJ/cm^2.

In the reaction-limited regime, neutralization follows rate equation (8). Thus, the remaining relative quencher concentration at the end of PEB of time *t* is

$$q(t) = h(t) - \delta_0 = \frac{q_0 \delta_0 e^{-k_Q G_0 \delta_0 t}}{(q_0 + \delta_0) - q_0 e^{-k_Q G_0 \delta_0 t}} \tag{15}$$

Since the quenching rate constant is finite, there may be incomplete quenching even in the reaction-limited regime. Figure 2 shows the amount of quencher remaining after PEB as a function of δ_0.

The quenching reaction during PEB is expected to be diffusion limited. The PROLITH SRM was run for an open-frame exposure using the baseline parameters of Table I, varying exposure dose. Additionally, acid and base diffusivity were varied, keeping the two diffusivities equal to each other. For each dose, the mean acid concentration in the volume was extracted from at least 10,000 trials. From this value, the reaction-limited value of the acid concentration, calculated from equation (15), was subtracted. The difference, plotted in Figure 1, measures how much slower the quenching reaction is in the diffusion-limited case compared to the ideal reaction-limited case. As expected, increasing the diffusion length in

PROLITH makes the results closer to the ideal reaction-limited case. Also, the impact of being in the diffusion-limited region on the mean acid concentration is only noticeable for small values of *h*, in the range of about 0.15 or less when the diffusion length is 5 nm or greater.

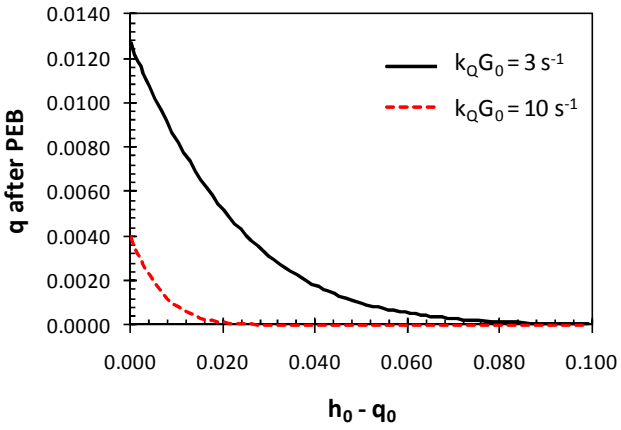

Figure 2. Reaction-limited quenching will give incomplete quenching for small $\delta_0 \equiv h_0 - q_0$ and/or small k_Q. In this plot, q_0 = 0.25 and the PEB time is 25 s.

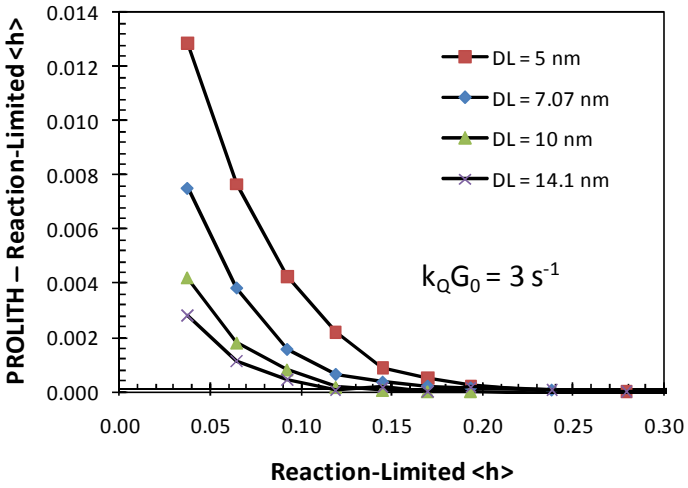

Figure 3. Comparison of the mean acid remaining after PEB as calculated by PROLITH to the result for a reaction-limited case (using the base-line parameters of Table I). As the diffusion length (DL) increases, the PROLITH stochastic model results approach the reaction-limited results.

To further elucidate the impact of diffusion, the quenching rate constant was increased by more than a factor of 30, to 500 nm^3/s, and the PROLITH SRM simulations were repeated. At this value, k_QG_0 = 100 s^{-1} and the reaction limited value of *h* is effectively $h = \delta_0 \equiv h_0 - q_0$. The results are shown in Figure 4. For the case of a 5-nm diffusion length, the impact of a higher reaction rate constant is significant.

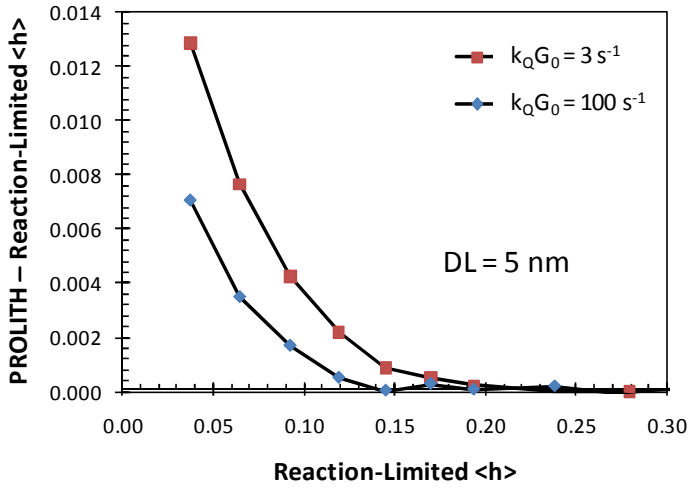

Figure 4. Comparison of the mean acid remaining after PEB as calculated by PROLITH to the result for the reaction-limited case, when k_Q = 15 and 500 nm^3/s and the diffusion length is 5 nm.

It is desirable to have an analytical expression to predict the amount of unreacted quencher at the end of PEB when in the diffusion-limited regime. By looking at the results of PROLITH SRM simulations over a range of quenching rate constants and various acid and base diffusion lengths, it was observed that equation (15) would fit the data within the statistical uncertainty of the data when k_Q was adjusted to provide the best fit. Calling this best-fit value $k_{Q\text{-}eff}$, Figure 5 shows this effective quenching rate constant as a function of diffusivity (D_H) for both large and small values of k_Q. These results are reasonably well fit by the following empirical expression:

$$k_{Q-eff} = k_Q\left(1 - e^{-11.0\sqrt{D_H}/k_Q}\right) \tag{16}$$

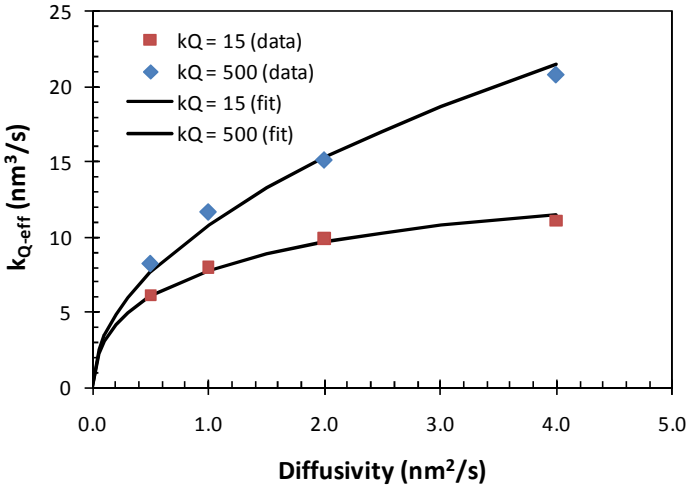

Figure 5. The effective acid-base quenching rate constant as a function of the actual k_Q and the diffusion length. All other parameters as in Table I. The fit (solid lines) to the simulation results (symbols) is given by equation (16).

IV. SIMULATION RESULTS –ACID CONCENTRATION UNCERTAINTY

The open-frame simulations described above were also used to determine the standard deviation of the acid concentration after PEB. A typical result is shown in Figure 6. As expected, the added uncertainties of the random placement of quencher and the probabilistic nature of acid-base diffusion and reaction leads to increasing acid uncertainty as the PEB proceeds. At exposure doses just large enough to produce an excess of acid over quencher, the final acid uncertainty becomes extremely high.

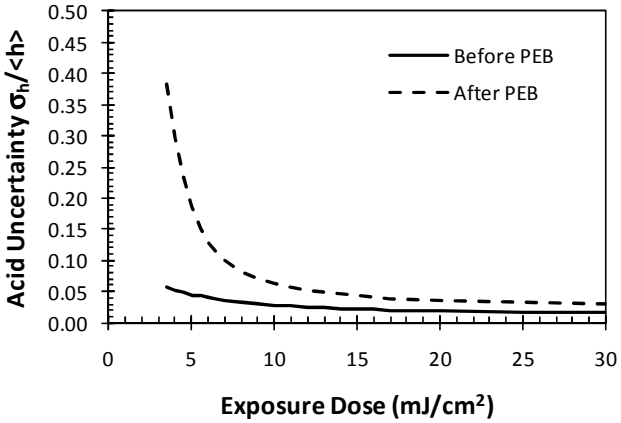

Figure 6. The relative acid uncertainty for an open frame exposure (volume = 50nmX50nmX10nm) before and after PEB. All parameters as in Table I.

An empirical expression was found to fit the data of relative acid uncertainty after PEB as a function of exposure dose, initial PAG concentration, and initial quencher concentration.

$$\left(\frac{\sigma_h}{\langle h\rangle}\right)^2_{After\ PEB} = \left(\frac{\sigma_{h_0}}{\langle h_0\rangle}\right)^2_{Before\ PEB} + \frac{4.0\langle q_0\rangle^{0.64}}{\langle h\rangle\langle n_{0-PAG}\rangle}\left[\frac{1}{\langle h\rangle} - 0.2\right] \qquad (17)$$

An example fit is shown in Figure 7. At the lowest exposure dose, the empirical expression overestimates the relative acid uncertainty. At all other doses, the fit is good. Thus, equation (17) applies to the case of complete quenching, since as we have seen in the previous section the lowest doses do not produce complete quenching. The interpretation of the form of this equation, and the meaning of the empirical constants, is hard to establish.

V. DISCUSSION AND CONCLUSIONS

The stochastic $A + B \rightarrow 0$ is well known to be a very difficult problem. Using the PROLITH Stochastic Resist Model, a first attempt at quantifying this problem for the case of three-dimensional acid-base quenching has been made. Incomplete quenching is a result of both a finite diffusivity (not every base quencher comes in contact with an acid) and a finite reaction rate constant (not every acid-base contact results in reaction). The mean acid and base concentrations in an open-frame exposure after PEB can be estimated by the reaction-limited rate equation (15) when the reaction rate constant k_Q is replaced by an effective reaction-diffusion rate constant $k_{Q\text{-}eff}$. A very preliminary study has found a simple, approximate

relationship for $k_{Q\text{-}eff}$ as a function of acid diffusivity (base diffusivity is set equal to acid diffusivity here) and quenching reaction rate constant. The result, equation (16), does a good job of describing the stochastic simulations performed here. However, many more simulation conditions are required to confirm this result.

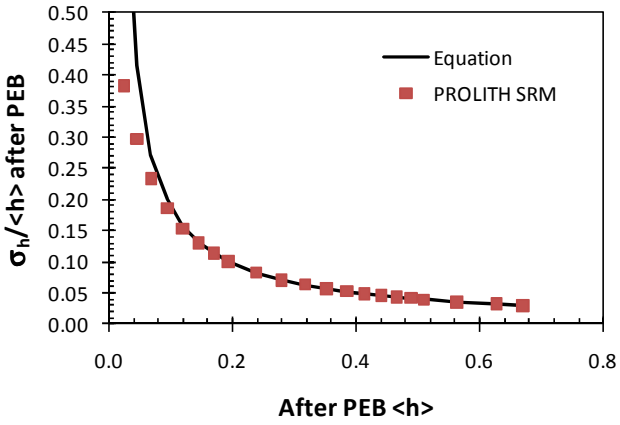

Figure 7. The relative acid uncertainty for an open frame exposure as simulated by PROLITH and fit by equation (17). All parameters as in Table I.

From the perspective of line-edge roughness, a more interesting result is the standard deviation of the acid concentration in the open frame after PEB. After many simulations using the PROLITH SRM, the empirical expression (17) was developed to fit the results. This expression is somewhat unsatisfying since its theoretical origins are not provided, and the physical significance of its three empirical constants have not been elucidated. Still, the expression allows for a quantitative prediction of how acid-base quenching increases the uncertainty is acid concentration.

Previous work has shown how acid uncertainty during PEB produces uncertainty in polymer protecting group concentration after PEB when no quencher is present.[6] Polymer deprotection responds to the time-average of the acid concentration during PEB. Thus, acid uncertainty will propagate to polymer protecting group uncertainty through this same time-average. As Figure 6 clearly shows, the acid uncertainty is a function of PEB time due to quenching. Thus, further work should explore this time-averaging effect in order to predict the impact of quenching on polymer protecting group concentration, and ultimately on line-edge roughness.

---

[1] C. A. Mack, "Line-Edge Roughness and the Ultimate Limits of Lithography", *Advances in Resist Technology and Processing XXVII, Proc.*, SPIE Vol. 7639, p. 763931 (2010).

[2] J. J. Biafore, M. D. Smith, S. Robertson, and T. Graves, "Mechanistic Simulation of Line Edge Roughness", *Advances in Resist Technology and Processing XXII, Proc.*, SPIE Vol. 6519, p. 65190Y (2007).

[3] D. ben-Avraham and S. Havlin, Diffusion and Reactions in Fractals and Disordered Systems, Cambridge University Press, Cambridge (2000).

[4] A. M. Turing, "The Chemical Basis of Morphogenesis" *Phil. Transact. Royal Soc. Series B*, Vol. 237, No. 641, pp. 37–72 (1952).

[5] C. A. Mack, J. W. Thackeray, J. J. Biafore, M. D. Smith, "Stochastic Exposure Kinetics of EUV Photoresists: A Simulation Study", *Extreme Ultraviolet (EUV) Lithography II, Proc.*, SPIE Vol. 7969 (2011).

[6] C. A. Mack, Fundamental Principles of Optical Lithography: The Science of Microfabrication, J. Wiley & Sons, London, pp. 247-253 (2007).